Photon Scattering by the Giant Magnetic Dipole States in ^{12}C, ^{24}Mg, and ^{28}Si†

H. W. KUEHNE,* P. AXEL, AND D. C. SUTTON
Department of Physics, University of Illinois, Urbana, Illinois
(Received 25 May 1967)

Photons, defined in energy to about 1% with the aid of a bremsstrahlung monochromator, were scattered by isolated energy levels in C, Mg, and Si. Parameters for the six observed levels are:

Isotope	Energy (MeV)	Γ_0^2/Γ (eV)	Γ_0/Γ	$B(M1)/(e\hbar/2M_pc)^2$
C^{12}	15.11	36	1	0.93
Mg^{24}	10.66±0.02	14	0.8	1.21
Si^{28}	11.42±0.02	23	1	1.33
Si^{28}	12.33±0.03			
Mg^{24}	9.92±0.03	3.0	0.5	0.49
Mg^{26}	10.07±0.05	4.2		≥0.36

The 15.11-MeV level in C^{12}, the 9.92- and 10.66-MeV levels in Mg^{24}, and the 11.42-MeV level in Si^{28} are $T=1$, $T_z=0$ analogs of low-lying 1+ states in the neighboring odd-odd nuclei. These levels exhaust most of of the magnetic dipole transition strength of the respective nuclei, and therefore give information about the expectation value of $\mathbf{l}\cdot\mathbf{s}$ in the ground state.

I. INTRODUCTION

THE resolution of the University of Illinois bremsstrahlung monochromator[1,2] was exploited to obtain new information about the large photon scattering previously associated with C, Mg, and Si between about 10 and 15.1 MeV. The discrete levels responsible for the scattering in Mg and Si were identified unambiguously. In addition, level widths were determined more reliably, and previously reported contradictory conclusions about level parameters were explained. The energy levels involved are of particular interest for two reasons: They correspond to the "giant magnetic dipole resonance," and they are the isobaric analog states of several low-lying states in the neighboring odd-odd nuclei.

Resonance fluorescence experiments involving isolated energy levels can give information about both the partial radiative width of the level to the ground state Γ_0 and the total level width Γ. The possibility of doing such experiments with γ rays from a bremsstrahlung continuum was suggested by Schiff,[3] who also stressed some of the difficulties. After an intervening decade (during which numerous experimental improvements were made, particularly in NaI detectors and multichannel analyzers), resonant scattering was reported[4] from the 15.1-MeV level in C^{12}. Hayward and Fuller[5] determined the widths of this level by analyzing their scattering and resonant absorption measurements. Although many subsequent fluorescence experiments were performed with bremsstrahlung (on the 15.1-MeV level,[6–10] on Mg near 10.5 MeV,[7–13] and on Si near 11.4 MeV[9,10,12–14]), considerable uncertainty remained about the widths. A preliminary experiment reported with the bremsstrahlung monochromator[15] made it clear that the improved resolution reduced the ambiguities considerably. Resonance fluorescence experiments have also been performed on the 15.1-MeV level using a $\mathrm{Li}(p,\gamma)$ source of γ rays.[16,17]

Precise resonance fluorescence experiments are particularly interesting because they both supplement and are supplemented by inelastic-electron-scattering ex-

† Supported by the U. S. Office of Naval Research under Contract N00014-67-A-0305-0005.
* Now at Douglas Aircraft Company. The material in this paper is based, in part, on a thesis submitted in 1964 in partial fulfillment of the requirements for the degree of Ph.D. in Physics.
[1] J. S. O'Connell, P. A. Tipler, and P. Axel, Phys. Rev. **126**, 228 (1962).
[2] P. A. Tipler, P. Axel, N. Stein, and D. C. Sutton, Phys. Rev. **129**, 2096 (1963).
[3] L. I. Schiff, Phys. Rev. **70**, 761 (1946).
[4] E. G. Fuller, E. Hayward, and N. Svantesson, Bull. Am. Phys. Soc. **1**, 21 (1956).
[5] E. Hayward and E. G. Fuller, Phys. Rev. **106**, 991 (1957).
[6] E. L. Garwin, Phys. Rev. **114**, 143 (1959).
[7] M. Langevin and A. Bussiere de Nercy, J. Phys. Radium **20**, 831 (1959).
[8] A. Bussiere de Nercy and M. Langevin, J. Phys. Radium **21**, 293 (1960).
[9] A. Bussiere de Nercy, Ann. Phys. (Paris) **6**, 1379 (1961). Note that this is a thesis which summarizes and reinterprets the experiments reported in Refs. 7, 8, 11, and 14.
[10] F. D. Seward, Phys. Rev. **125**, 335 (1962).
[11] A. Bussiere de Nercy, Compt. Rend. **250**, 1252 (1960).
[12] R. A. Tobin, Phys. Rev. **120**, 175 (1960).
[13] M. Sugawara, J. Phys. Soc. Japan **16**, 1857 (1961).
[14] A. Bussiere de Nercy, J. Phys. Radium **22**, 119 (1961).
[15] P. Axel, F. T. Kuchnir, H. W. Kuehne, K. Min, N. Stein, and D. C. Sutton, Bull. Am. Phys. Soc. **6**, 440 (1961).
[16] S. S. Hanna and R. E. Segel, Proc. Roy. Soc. (London) **A259**, 267 (1960).
[17] H. Schmid and W. Scholz, Z. Physik **175**, 430 (1963).

periments.[18–24] Inelastic-electron-scattering experiments should determine Γ_0 quite well, once the validity of the approximations used in the analysis are established. Resonance fluorescence experiments, on the other hand, can determine Γ_0^2/Γ quite precisely, and Γ_0/Γ with more difficulty. Values of Γ_0 reported from inelastic-electron-scattering measurements had appeared disquietingly low compared to what had been interpreted as reliable values from resonance fluorescence experiments. The values obtained in this improved resonance fluorescence experiment are in excellent agreement with the electron-inelastic-scattering results,[19–23] and thereby give strong support to the analysis procedures used to interpret those results.

II. THE RELATION BETWEEN LEVEL PARAMETERS AND FLUORESCENCE MEASUREMENTS

The energy dependence of the photon excitation of a discrete quantum state is well known,[25–27] but will be summarized below to define terms and to indicate exactly how the level parameters were obtained from the data. It will be shown that despite a complicated dependence of the cross section on the laboratory energy of the γ ray, the energy integrated scattering due to one level defines Γ_0^2/Γ for that level. If the scattering sample is not infinitely thin, an auxiliary absorption measurement is needed to correct for self-absorption. The auxiliary absorption measurement can also be used to obtain a value of Γ_0/Γ but most measurements yield only approximate values. For the low-Z nuclei of interest in this paper, the atomic absorption can be treated as a small correction. This simplifies the analysis considerably because the convenient curves available for analyzing neutron resonances can be used directly. This approximation also makes it possible to show graphically (in Figs. 1 and 2 below) the precision attainable from fluorescence measurements.

A. Thin Samples; Negligible Self-Absorption

In the center-of-mass coordinate system, the absorption cross section σ_a for a γ ray of energy E' by a nucleus with a level resonant at E_R' is particularly simple:

$$\sigma_a(E')=\sigma_a^0\frac{1}{1+[(2/\Gamma)(E'-E_R')]^2}\equiv\sigma_a^0\left(\frac{1}{1+y^2}\right). \quad (1)$$

The peak cross section σ_a^0 is very large for photon energies near 10 MeV:

$$\sigma_a^0=2\pi\lambda\!\!\!^{-2}\left(\frac{2I_f+1}{2I_g+1}\right)\frac{\Gamma_0}{\Gamma} \quad (2a)$$

$$=73\text{ b}\left(\frac{\Gamma_0}{\Gamma}\right)\left(\frac{10\text{ MeV}}{E_R'}\right)^2\left(\frac{2I_f+1}{3(2I_g+1)}\right). \quad (2b)$$

I_f is the spin of the final (excited) state, I_g is the ground-state spin, and the bracketed spin factor in Eq. (2b) reduces to unity of a 0+ target is excited by dipole radiation.

One important difference between the laboratory and center-of-mass system is due to the recoil energy of a nucleus ΔE; if the absorbing nucleus were stationary, the resonant γ ray energy in the laboratory E_R would be greater than E_R' by ΔE:

$$\Delta E=E_R-E_R'=\frac{(\hbar k)^2}{2AM}=2.24\text{ keV}\left(\frac{24}{A}\right)\left(\frac{E_R}{10\text{ MeV}}\right)^2, \quad (3)$$

where A is the mass number and M the nucleon mass. Because the energy shift due to recoil is considerably larger than the level widths discussed below, nuclear absorption is negligible for γ rays which have been resonantly scattered by nuclei.

The dependence of the cross section on the energy in the laboratory is complicated considerably by the thermal motion of the absorbing nuclei. It is usually assumed that these nuclei have a Maxwellian velocity distribution corresponding to a gas with an effective absolute temperature T. The normalized probability $W(E,E')$ that a γ ray with laboratory energy E has a center-of-mass energy E' can be expressed in terms of the recoil energy ΔE and a Doppler width Δ:

$$\Delta=\frac{E}{c}\left(\frac{2kT}{AM}\right)^{1/2}=14\text{ eV}\left(\frac{E}{10\text{ MeV}}\right)\left(\frac{24}{A}\right)^{1/2}\times\left(\frac{T}{300}\right)^{1/2} \quad (4)$$

$$W(E,E')=\frac{1}{\Delta\pi^{1/2}}\exp[-(E-\Delta E-E')^2/\Delta^2]. \quad (5)$$

(In a solid, the effective temperature T is equal to or greater than the actual temperature depending on the Debye temperature.[27–29] For temperatures much above

[18] W. C. Barber, Ann. Rev. Nucl. Sci. **12**, 1 (1962); J. Goldemberg and R. H. Pratt, Rev. Mod. Phys. **38**, 311 (1966).
[19] W. C. Barber, F. Berthold, G. Fricke, and F. E. Gudden, Phys. Rev. **120**, 2081 (1960).
[20] R. Edge and G. A. Peterson, Phys. Rev. **128**, 2750 (1962).
[21] W. C. Barber, J. Goldemberg, G. A. Peterson, and Y. Torizuka, Nucl. Phys. **41**, 461 (1963).
[22] F. Gudden, Phys. Letters **10**, 313 (1964).
[23] O. Titze and E. Spamer, Z. Naturforsch **21**, 1504 (1966).
[24] Experiments performed with the Naval Research Laboratory Linac according to L. W. Fagg (private communication).
[25] H. A. Bethe and G. Placzek, Phys. Rev. **51**, 450 (1937).
[26] H. A. Bethe, Rev. Mod. Phys. **9**, 69 (1937).
[27] See the review article by F. R. Metzger, Progr. Nucl. Phys. **7**, 53 (1959).
[28] W. E. Lamb, Jr., Phys. Rev. **55**, 190 (1938).
[29] J. Rainwater, in *Encyclopedia of Physics*, edited by S. Flügge (Springer-Verlag, Berlin, 1957), Vol. 40.

the Debye temperature, the effective temperature is essentially equal to the actual temperature; for very low temperatures, the effective temperature falls to the Debye temperature.)

The absorption cross section in terms of laboratory energy E can be obtained by substituting Eq. (5) in Eq. (1):

$$\sigma_a(E)=\sigma_a{}^0\frac{1}{\Delta\pi^{1/2}}\int_0^\infty dE'\frac{\exp[-(E-\Delta E-E')^2/\Delta^2]}{1+y^2} \quad (6a)$$

$$\cong\sigma_a{}^0\frac{\Gamma}{2\Delta\pi^{1/2}}\int_{-\infty}^{+\infty}dy \times\frac{\exp[-(E-\Delta E-E')^2/\Delta^2]}{1+y^2}. \quad (6b)$$

Equation (6) is usually expressed in abbreviated notation in terms of a tabulated function $\psi(x,t)$:

$$\sigma_a(E)=\sigma_a{}^0\psi(x,t), \quad (7a)$$

where

$$x=2(E-E_R)/\Gamma \quad (7b)$$

and

$$t=(\Delta/\Gamma)^2. \quad (7c)$$

The scattering cross section $\sigma_s(E)$ is simply the product of the absorption cross section and the branching ratio Γ_0/Γ:

$$\sigma_s(E)=(\Gamma_0/\Gamma)\sigma_a(E). \quad (8)$$

The scattering observed in a poor resolution experiment is affected by the complicated energy dependence [of Eq. (6)] only because of self-absorption in the scatterer. If a very thin sample were used, the scattering would be simply proportional to the energy integrated scattering cross section I_s, independent of Δ or Δ/Γ:

$$I_s=\int\sigma_s(E)dE=\frac{\pi}{2}\Gamma\sigma_a{}^0\frac{\Gamma_0}{\Gamma}=\frac{\pi}{2}\sigma_a{}^0\Gamma_0 \quad (9a)$$

$$=1.15\text{ MeV mb}\frac{\Gamma_0{}^2/\Gamma}{10\text{ eV}}\left(\frac{10\text{ MeV}}{E_R}\right)^2\left(\frac{2I_f+1}{3(2I_g+1)}\right). \quad (9b)$$

Equation (9b) indicates explicitly that the scattering observed from a thin sample could determine $\Gamma_0{}^2/\Gamma$. The next section will show how an auxiliary resonant absorption experiment can determine the self-absorption correction, and thereby make it possible to determine I_s or $\Gamma_0{}^2/\Gamma$ with good precision.

B. Self-Absorption Corrections in Thicker Samples

Nuclear resonant absorption occurs only in the incident beam, and is essentially always caused by only the isotope responsible for the scattering. Atomic absorption, on the other hand, is caused by all of the isotopes and occurs in both the incident and scattered beam. Fortunately, the corrections due to atomic scattering were small, and could be calculated to sufficient accuracy despite simplifying approximations. The remainder of this section will deal with only the effects of, and corrections for, the resonant nuclear scattering.

It is convenient to define a self-absorption correction factor $\mathcal{S}$, which is the ratio of the actual number of scattering events to the number expected if there were negligible attenuation of the incident beam. This complicated factor $\mathcal{S}$ can be expressed in terms of the cross section and $\mathfrak{N}$, the number of atoms per unit area perpendicular to the incident beam:

$$\mathcal{S}I_s=\int dE\sigma_s(E)\left\{\frac{1-\exp[-\mathfrak{N}\sigma_a(E)]}{\mathfrak{N}\sigma_a(E)}\right\}. \quad (10)$$

Although $\mathcal{S}$ depends on the resonance energy, the spins Γ_0/Γ and Δ/Γ, as well as on $\mathfrak{N}$, it will be adequate to show only the dependence on $\mathfrak{N}$ explicitly.

The counting rate observed from a scatterer, of thickness $\mathfrak{N}_s$, when no absorber is in the beam C_{NA} can be written as

$$C_{NA}=F\mathfrak{N}_s\mathcal{S}(\mathfrak{N}_s)I_s, \quad (11)$$

where the constant F includes detection efficiency and normalization to unit incident flux. Thus, a scattering measurement with a single scattering sample determines the product of two unknown factors $\mathcal{S}(\mathfrak{N}_s)$ and I_s. $\mathcal{S}(\mathfrak{N}_s)$ is plotted as a function of $\mathfrak{N}_s\sigma_a{}^0$ in Fig. 1, with Δ/Γ as a parameter. The values for Fig. 1 were obtained from the graphs[29,30] used to interpret slow neutron resonance experiments. (In terms of A, the usual area parameter,[29] $\mathcal{S}$ can be written simply as, $\mathcal{S}=[2/\pi]\times[A/\mathfrak{N}\sigma_0\Gamma]$.) Equation (2b) makes it clear that even if the spins, energy, and responsible isotope are known, the value of abscissa, $\mathfrak{N}_s\sigma_a{}^0$, is proportional to the unknown fraction Γ_0/Γ.

$\mathcal{S}(\mathfrak{N})$ can be found by using Fig. 1 to interpret measurements made with scattering samples of different thickness. A more precise way of finding $\mathcal{S}(\mathfrak{N})$ involves the use of an absorber of thickness $\mathfrak{N}_a$ in "good geometry." Because all the detected interactions originate in the scatterer, they can be expressed as the difference between all of the interactions and those occurring in the absorber. The observed scattering with this absorber in place C_A is

$$C_A=FI_s[(\mathfrak{N}_s+\mathfrak{N}_a)\mathcal{S}(\mathfrak{N}_s+\mathfrak{N}_a)-\mathfrak{N}_a\mathcal{S}(\mathfrak{N}_a)]. \quad (12)$$

The value of $\mathcal{S}(\mathfrak{N}_s)$ can be determined by measuring the ratio R:

$$R=(C_{NA}-C_A)/C_{NA}. \quad (13)$$

[30] We are indebted to the neutron physics group at Brookhaven National Laboratory, who made large copies of these graphs available. These graphs are reproduced in Ref. 29.

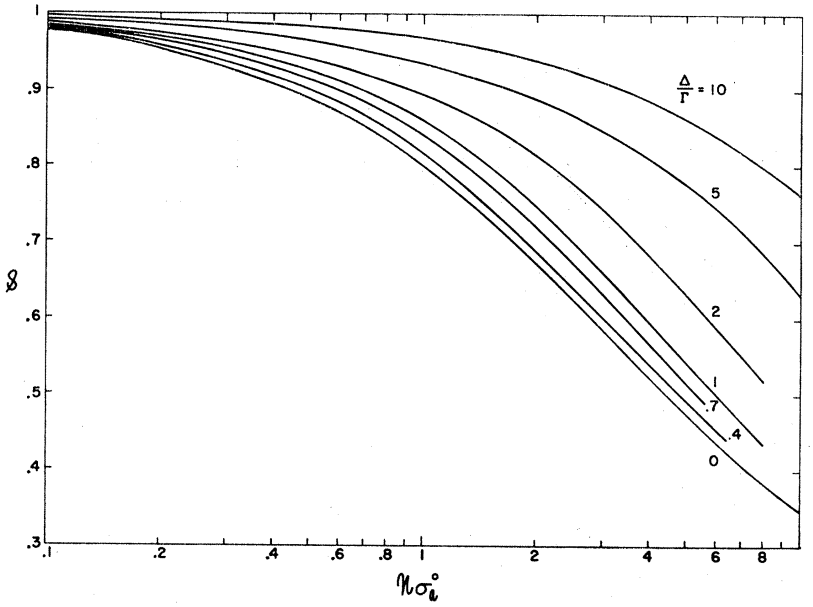

FIG. 1. The self-absorption correction factor $\mathcal{S}$. The correction factor $\mathcal{S}$ of Eq. (10) is shown as a function of $\mathfrak{N}\sigma_a^0$ [see Eq. (2)] for different values of Δ/Γ. Larger values of Δ/Γ imply broader resonances which result in less self-absorption so that the correction factor is closer to 1.

From Eqs. (11) and (12), R can be written as

$$R=\frac{\mathfrak{N}_s\mathcal{S}(\mathfrak{N}_s)+\mathfrak{N}_a\mathcal{S}(\mathfrak{N}_a)-(\mathfrak{N}_a+\mathfrak{N}_s)\mathcal{S}(\mathfrak{N}_a+\mathfrak{N}_s)}{\mathfrak{N}_s\mathcal{S}(\mathfrak{N}_s)}. \quad (14)$$

For our measurements we chose to use $\mathfrak{N}_a=\mathfrak{N}_s=\mathfrak{N}$, in which case R reduces to

$$R(\mathfrak{N}_a=\mathfrak{N}_s)=\frac{2[\mathcal{S}(\mathfrak{N})-\mathcal{S}(2\mathfrak{N})]}{\mathcal{S}(\mathfrak{N})}. \quad (15)$$

Figure 2 shows $\mathcal{S}(\mathfrak{N})$ as a function of $R(\mathfrak{N}_a=\mathfrak{N}_s)$ for various values of Δ/Γ. Figure 2 makes it clear that a determination of the ratio R tends to determine the self-absorption correction $\mathcal{S}$ within small limits even if Δ/Γ is quite uncertain.

The obvious correction for atomic absorption in the absorber was an adequate correction for all of the atomic absorption effects. Inasmuch as the atomic and nuclear absorption are separable in the absorber, the measured value $C_{\text{A measured}}$, can be corrected to what it would have been if there were no atomic absorption in the absorber:

$$C_A=C_{\text{A measured}}\exp(\mathfrak{N}_{\text{atomic}}\sigma_{\text{atomic}}). \quad (16)$$

The use of Eq. (16) to define C_A for Eq. (13) corrected for atomic absorption to better than 0.5%.

C. Final Determination of Level Parameters

The measurements of the scattering, C_{NA}, and the resonant absorption reduction factor R contain some information about Γ_0/Γ and Δ/Γ as well as the more precise information about Γ_0^2/Γ discussed in the preceding paragraphs. An indication of the limits imposed by the absorption factor R can be seen in Fig. 3, which shows the value of $\mathfrak{N}_s\sigma_a^0$ implied by different values of R with Δ/Γ as a parameter. The family of curves in

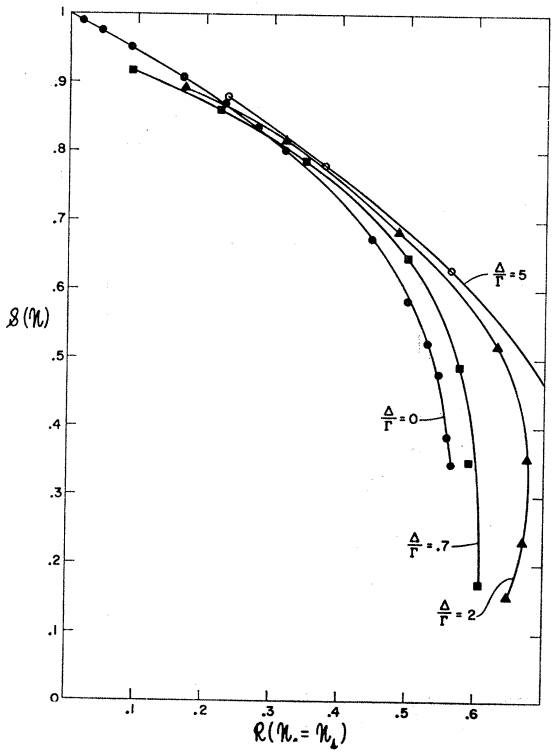

FIG. 2. The relation between the correction factor $\mathcal{S}$ and the observed resonant absorption R. The curves are drawn for various values of Δ/Γ, but all correspond to equal thicknesses of absorber and scatterer, as in Eq. (15). They show that a measurement of R [in Eq. (15)] can be used to determine $\mathcal{S}(\mathfrak{N})$ rather precisely even if Δ/Γ is uncertain.

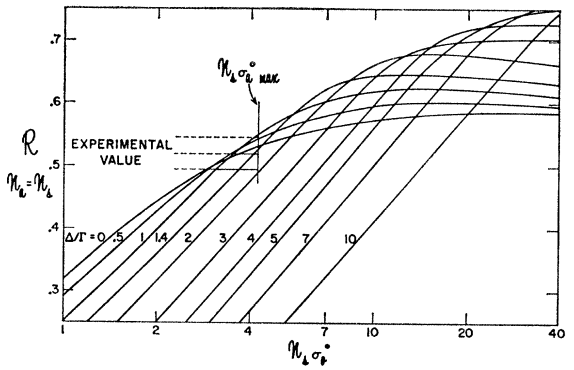

FIG. 3. The relationship between $R(\mathfrak{N}_a=\mathfrak{N}_s)$ and $\mathfrak{N}_s\sigma_a{}^0$ for different values of Δ/Γ. An absorption measurement which determines R defines a horizontal band; the band corresponding to the 10.66-MeV level in Mg^{24} is shown in the figure as an illustration. This type of measurement alone can set only a lower limit on Γ_0/Γ. The value $\Gamma_0/\Gamma=1$ substituted into Eq. (2) defines the upper limit of $\mathfrak{N}_s\sigma_a{}^0$ if the sample thickness and level spins are known. The vertical line shown on the figure is the maximum value appropriate to the 10.66 MeV level in Mg^{24} with the sample thickness used, assuming $I_f=1$.

Fig. 3 is valid for equal absorber and scatterer (i.e., $\mathfrak{N}_a=\mathfrak{N}_s$); the illustrative restrictions imposed by a measured ratio are shown for Mg^{24}. For the strong levels we studied, the condition $(\Gamma_0/\Gamma)\leq 1$ set an important upper limit on $\mathfrak{N}_s\sigma_a{}^0$.

The complete determination of the level parameters involves combining the scattering and absorption data on a $\mathfrak{N}\sigma_a{}^0$-versus-Δ/Γ plane as is done in Fig. 4. The scattering data select the region S whose general appearance can be understood easily. The parameter combination $\Gamma_0{}^2/\Gamma$ determined by the scattering could

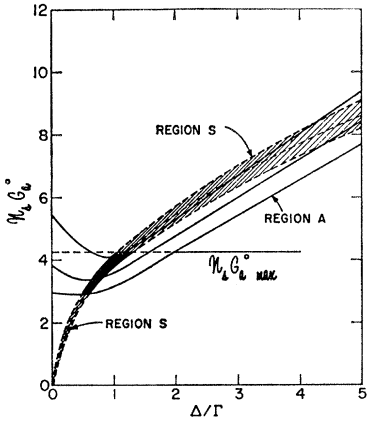

FIG. 4. The determination of Γ_0 and Γ using scattering and absorption data for the 10.66-MeV level in Mg^{24}. The shaded area defined by the dashed curves indicates the values of $\mathfrak{N}\sigma_a{}^0$ and Δ/Γ which are consistent with the elastic scattering caused by the 10.66-MeV level in Mg^{24}. (The center curve is the best experimental value while the other two curves represent the estimated experimental error.) The solid curves indicate the locus of values consistent with the absorption measurement. The horizontal line, labeled $\mathfrak{N}_s\sigma_a{}^0{}_{\max}$ corresponds to $\Gamma_0/\Gamma=1$. The blackened area represents the region simultaneously consistent with both the scattering and the absorption measurements.

be explained by a variety of values, Γ_0, Γ_0/Γ, and Δ/Γ_0. If Γ_0 were much larger than $\Gamma_0{}^2/\Gamma$, Γ/Γ_0 would have to be much larger than 1 so that Δ/Γ would be small. On the other hand, if $\Gamma_0=\Gamma=\Gamma_0{}^2/\Gamma$, both Γ_0 and Γ would have a minimum value while Δ/Γ would have a corresponding maximum. The region A selected by the absorption data has a more complicated dependence on Γ_0/Γ and Δ/Γ, as implied by Fig. 3. The condition $\Gamma_0/\Gamma\leq 1$ corresponds to defining maximum values of $\mathfrak{N}\sigma_a{}^0$ which depend on the multipolarity because of the spin factor in Eq. (2).

Figure 4 illustrates, in part, the difficulty usually associated with determining Γ_0 or Γ_0/Γ with precision. Most of the parameters reported in this paper are relatively precise because the levels are so strong that the observed absorption places a lower limit on Γ_0/Γ independent of the exact energy dependence of the cross section (i.e., independent of Δ/Γ). If Δ/Γ is either much less than 1 (which is extremely rare for levels which cannot emit nucleons) or much greater than 1 (which is the usual case), an absorption measurement can determine Γ_0/Γ or Γ_0/Δ, respectively. However, for intermediate values of Δ/Γ, the absorption is relatively insensitive to Γ_0/Γ or Γ_0/Δ. Previous experiments have attempted to overcome this difficulty[5–7] by using several absorbers, including some that are quite thick. However, this type of experiment requires very high precision and is doomed to failure if there are some weak levels unresolved from the strong one of interest. Another approach has been to obtain approximate level parameters with the aid of astute, but generally unjustifiable assumptions[12,13]; the resulting parameters have been widely misinterpreted as having higher reliability than the original authors would have claimed.

III. EXPERIMENTAL TECHNIQUES AND RESULTS

A. The Bremsstrahlung Monochromator

The equipment used was essentially the same as that described earlier.[1,2] An electron beam of energy E_β was bent by a magnet D and was refocused on a thin bremsstrahlung converter which was in the source position of a spectrometer magnet, S. The dispersion of the incident electron beam was about 0.25%/cm, while the dispersion of the spectrometer was about 1%/cm. Less than 0.1% of the electrons of energy E_β formed a gamma ray with $E_\gamma\geq 0.001\ E_\beta$. The formation of a γ ray of particular energy, E_γ, was announced by the detection of the corresponding electron of energy, E_e, in the focal plane of the spectrometer such that $E_\gamma=E_\beta-E_e$.

γ rays scattered at 135° were detected by a 5-in.-diameter by 4-in. thick NaI detector. A scattered γ ray could be associated with an incident γ ray of known energy, E_γ (i.e., with a "tagged" γ ray), by requiring a coincidence (about 10 nsec) between an electron of

energy E_e and the scattered γ ray. In order to avoid chance coincidences, the beam intensity was kept low enough so that the detected electrons were about 2 μsec apart; with the 4% duty cycle this corresponded to about 1.4×10^4 "monochromatic" γ rays per second. Three identical plastic scintillators were used to detect the electrons so that this γ ray flux was available at three neighboring energies simultaneously.

The energy resolution of the incident γ-ray beam depended on E_β, E_e, the beam size, and the size of the plastic scintillators. When good resolution was important, as in the energy determination, 1.4-cm wide scintillators were used, whereas 1.95 cm scintillators were used in the resonant absorption measurements. For the energy measurements, the full width at half-maximum was about 100 keV, so that the 20 keV precision that was obtained was limited by statistical and calibration errors rather than by resolution. For the absorption measurements the critical experimental quantity is the fractional number of γ rays per unit energy interval at the nominal energy E_γ. This can be expressed conveniently by specifying the full width of the rectangular distribution that would give the same fractional number per unit energy. This full width was about 140 keV, which implies that there was 0.1γ/sec/eV when there were 1.4×10^4 tagged γ rays/sec.

The pulse heights of the scattered γ rays were displayed using a 100 channel analyzer, subdivided into four groups of 25. Three of the groups were used for the three different incident γ-ray energies while the fourth group of 25 channels was used to record chance coincidences. A typical spectrum of the scattered γ rays is shown in Fig. 5, which also shows the very low value of the chance coincidences. The energy resolution of the γ-ray detection system was very poor, with the result that inelastic scattering to the first excited state of Mg or Si would not have been resolved from the elastic scattering.

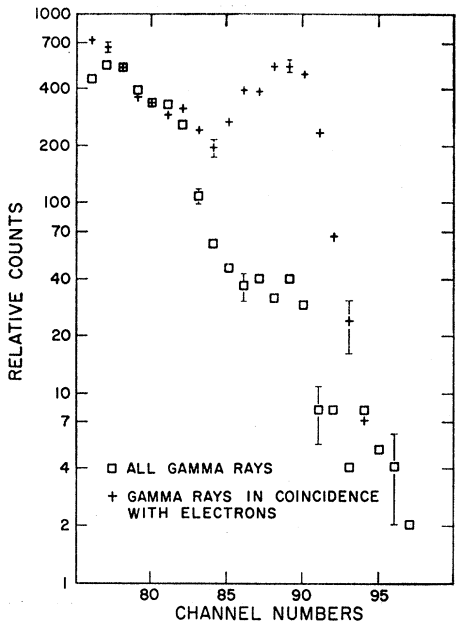

FIG. 5. Pulse-height distribution of the scattered γ rays with a Mg sample. The data represented by the crosses correspond to the γ rays detected in coincidence with electrons that defined the 10.66-MeV incident photon beam. The number of counts in channels 83–92 in about 16 h were 1392, of which 152 were chance coincidences. The chance coincidences were determined relatively precisely by detecting all of the scattered γ rays (without requiring coincidence with electrons). This spectrum normalized is shown by the squares; except for a small correction, these squares represent the chance coincidence background.

B. Level Survey and Energies

The energy region explored carefully in the natural Mg target is shown in Fig. 6. Levels which are so strong that they must be in Mg^{24} are obvious at 9.92 ± 0.03 MeV and 10.66 ± 0.02 MeV. An indication of the sensitivity of the technique can be obtained by noting the shoulder on the high-energy side of the 9.92-MeV line. Later absorption measurements made it clear that there was a level at about 10.07 ± 0.05 MeV which we attribute to Mg^{26}; a level in Mg^{24} with an integrated cross section of about 0.07 MeV mb would have produced a similarly suspicious, but inconclusive, peak.

Although the variation of monochromator resolution with energy is not known precisely, it is known well enough to guarantee that the 9.92-MeV line does not have a strong satellite[23] lower in energy by about 120 keV. If such a level exists in Mg^{24}, its integrated scattering cross section must be less than about 0.07 MeV mb. The 9.92-MeV line has a full width at half-maximum of 123 ± 15 keV, whereas our best estimate of the expected resolution is 112 keV.

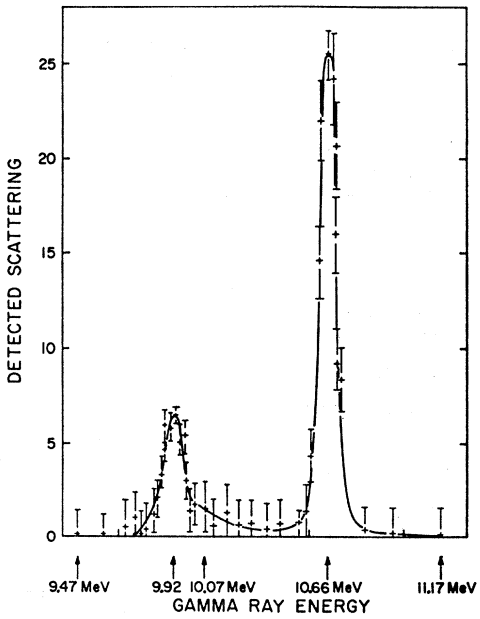

FIG. 6. Quasielastic γ-ray scattering observed with a Mg target. The scattering is called quasielastic because it includes any high-energy γ rays from inelastic scattering to low-lying levels.

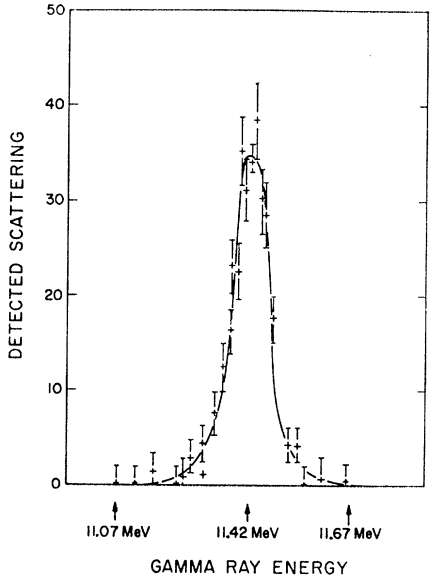

FIG. 7. Quasielastic γ-ray scattering observed with a Si target.

In the smaller energy interval covered with the Si target shown in Fig. 7, only the 11.42±0.02-MeV level could be seen. Levels in Si^{28} with integrated scattering cross sections of 0.1 MeV mb would have been seen away from the 11.42-MeV peak. The Si sample was also used to check quickly on a level reported[31] at 12.326 MeV. Using our calibration and a run of only 3 h we determined its energy as 12.33±0.03 MeV. (A crude estimate of the strength of this level gave $I_S=0.28$ ±0.10 MeV mb which is in reasonable agreement with the value of 0.23 MeV mb calculated from the parameters measured by Smith and Endt.[31])

C. Scattering and Resonant Absorption Measurements

For each level, two additional measurements were made. First, the scattering was measured using a 4 in.×6 in. sample parallel to the NaI detector. The detector subtended an angle of about 0.3 sr at the center of the sample. In addition, a second identical sample (making the same angle with the beam) was inserted in the beam as an absorber, and the resonant scattering from the original sample was measured. Typical counting rates, errors, and the inferred parameters are summarized in Table I.

The first line in Table I gives the isotope to which the observed level was assigned. These isotopic assignments were unambiguous for the first four levels because the strong absorption guaranteed that only the most abundant isotope could be responsible. On the other hand, the 10.07-MeV level was tentatively assigned to Mg^{26} because a similar γ ray had been observed following thermal neutron capture by Mg^{25}; this assignment is strongly supported by the observation of this level in the course of inelastic electron-scattering mea-

TABLE I. Scattering and resonant absorption results.

Responsible isotope	C^{12}	Si^{28}	Mg^{24}	Mg^{24}	Mg^{26}
Level energy (MeV)	15.11	11.42	10.66	9.92	10.07
Error (MeV)	stnd.	0.02	0.02	0.03	0.05
Thickness normal to beam (atoms/barn)	0.103	0.061	0.065	0.133	0.019
Scattering measurements (no absorber)					
Beam time (hours)	8	12	16	33	33
C_{NA} [(scattered γ)/sr (incident γ) eV]	10.18	6.37	5.06[a]	2.78[a]	0.64
Error [(scattered γ)/sr (incident γ) eV]	0.29	0.19	0.16	0.10	0.09
$\mathcal{S}I_S$ (MeV mb)	1.13	1.23	0.92	0.26	0.45
Percent error	6.0%	9.3%	9.3%	9.7%	14.3%
Scattering observed with absorber					
Beam time (hours)	14	26	28	77	77
$C_{A\ meas}$ [(scattered γ)/sr (incident γ) eV]	4.87	2.87	2.24[a]	1.07[a]	0.52
Error [(scattered γ)/sr (incident γ) eV]	0.16	0.09	0.08	0.05	0.04
R	0.503	0.517	0.520	0.545	0.090
Error	0.022	0.023	0.025	0.033	0.005
Δ (eV)	40	17.5	16.5	15.5	16.0
Derived parameters					
$\mathcal{S}$	0.63	0.61	0.60	0.60	0.94
Error in $\mathcal{S}$	0.04	0.05	0.06	0.07	0.04
I_S (MeV mb)	1.80	2.02	1.38[b]	0.35[b]	0.48
Γ_0^2/Γ (eV)	35.7	22.9	13.6[b]	3.0[b]	4.2
Γ_0/Γ	1.0	1.0	0.8	0.54	
Error in Γ_0/Γ	−0.2	−0.2	0.1	0.20	
Γ_0 (eV)	37.2[c]	22.9	17.0	5.6	

[a] Includes inelastic scattering to first excited state.
[b] Assumes 10% of observed 10.66-MeV counts and 25% of observed 9.92-MeV counts due to inelastic scattering.
[c] Uses $\Gamma_0/\Gamma=0.96$ from Ref. 32 together with the assumption that α decay and emission of lower energy γ rays are negligible.

[31] P. B. Smith and P. M. Endt, Phys. Rev. 110, 397 (1958).

surements[23,24] from separated Mg^{26}. The thickness of the scattering sample and the absorber perpendicular to the beam is given in atoms of the relvent isotope per barn. For the dominant isotopes, the sample thicknesses were of the order of 0.1 atom/b, which implies significant selfabsorption in the scatterer for peak cross sections of the order of 50 b, as might be inferred from Eq. (2).

The observed scattering, with and without an absorber, are normalized in Table I so that C_{NA} and $C_{\text{A measured}}$ are approximately equal to the number of scattered γ rays per sr at 135° when one γ ray is incident in each 1-eV energy region. To emphasize the convenience of this normalization, consider the entry 5.06 for the 10.66-MeV level in Mg^{24}. This means that the number of γ rays scattered into a steradian at 135° for this target is equal to the number of γ rays incident in a 5.06 eV energy bin. For our experiment, the flux incident on the sample was about 150 γ's per eV per hour, so that 2400 γ/eV are incident in 16 h. The entry 5.06 for Mg^{24} implies that 12 144 γ's would be scattered into a sr at 135°. Since the product of the solid angle and the detection efficiency was about 0.1, about 1200 scattered γ rays were detected.

The errors given for C_{NA} and $C_{\text{A measured}}$ are statistical errors only. Although the errors inherent in the normalization are larger, the smaller statistical errors are quoted to emphasize that these errors alone affect the relative values. (The higher precision of relative values applies to the measurements with and without absorber and to measurements made on different levels.) Larger errors are introduced into absolute values due to uncertainties in absolute detection efficiency and geometry. These larger errors are reflected in Table I in the values quoted for the integrated cross section $\mathcal{S}I_S$ (uncorrected for nuclear self-absorption).

The entry listed as $\mathcal{S}I_S$ in Table I is 11.2 times the apparent energy integrated cross section at 135° (differential in angle). The factor $\mathcal{S}$ is a reminder that no correction has been made for nuclear resonance absorption. The values given are only slightly greater than 11.2 times C_{NA} divided by the sample thickness; the discrepancy represents an approximate correction for atomic absorption.

The only significant source of error in $\mathcal{S}I_S$ which is not included in the estimates given in Table I is that associated with the possible contribution of inelastic scattering to the detected scattered radiation that was interpreted as elastic for the entries in the upper portion of Table I. An estimate of the possible inelastic scattering was made by comparing the spectrum of the scattered γ rays with the spectrum associated with a monoenergetic incident γ ray. This comparison is shown in Figs. 8(a), 8(b), and 8(c) for the levels in Si^{28} and Mg^{24}. Figure 8(a) shows that the scattered γ-ray points agree well with the curve which is the shape measured for 11.42-MeV incident γ rays. On the other hand, the solid curves in Figs. 8(b) and 8(c) do not fit the data as well. In these cases, the dashed curves (which include contributions from inelastic scattering to the first excited state) fit the scattering data better. In deriving the level parameters, it was assumed that the observed 135° scattering had 10% and 25% inelastic contributions for the 10.66- and 9.92-MeV levels, respectively.

The resonance absorption counting rates $C_{\text{A measured}}$, given in Table I, have not been corrected for atomic

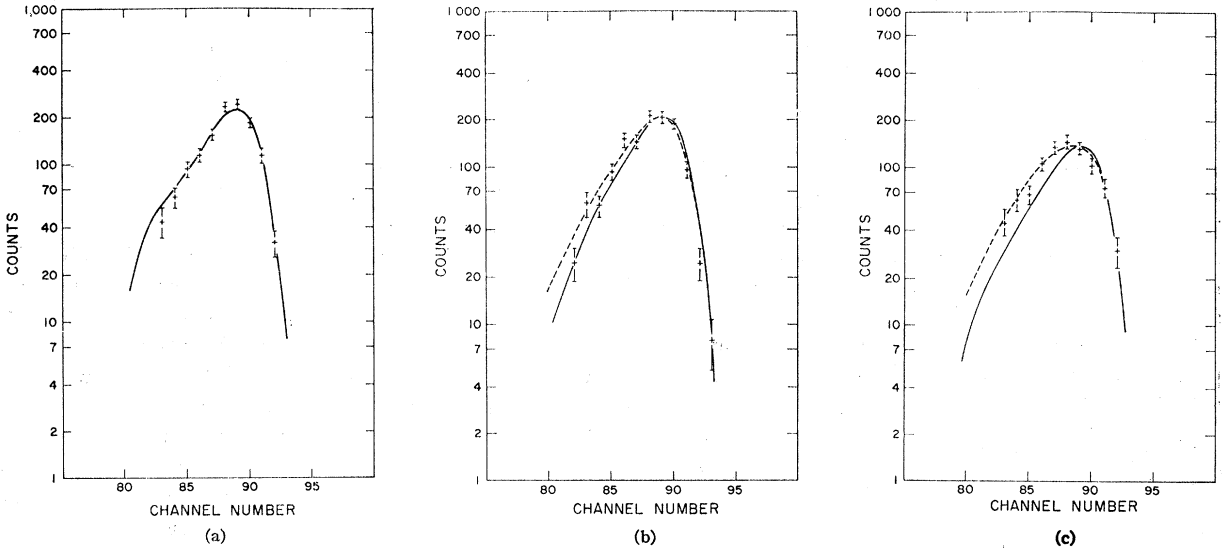

FIG. 8. Comparison of the pulse-height distribution of the scattered γ rays with the detector response for monoenergetic incident γ rays. The points are experimental (with chance coincidences subtracted), and the solid curves represent the normalized pulse-height distribution expected for monoenergetic incident γ rays. The dashed curves include different percentages of inelastic scattering to the first excited state. (a) Si target, 11.42 MeV; (b) Mg target, 10.66 MeV, dashed curve is 90% elastic; (c) Mg target, 9.92 MeV, dashed curve is 75% elastic.

absorption; these are experimental values expected if the absorber consists of the mixture of isotopes found naturally on earth. The ratio R in Table I was calculated after the correction of Eq. (16) was applied. The error in R is entirely statistical; systematic errors would not affect R significantly.

The remaining parameters given in Table I are derived from the measurements described. No attempt is made to include the errors for the final quantities because the errors to be assigned are ambiguous. A reasonable estimate of the errors in the absolute values of Γ_0^2/Γ is probably only slightly greater than the percentage error listed for SI_S. A reasonable estimate for the relative errors in ratios of values of Γ_0^2/Γ for different levels can be obtained by combining the errors cited for the corresponding S values. The errors quoted in the table for Γ_0/Γ are those which came from the measurements reported in this paper. However, as was mentioned earlier, these experiments are not particularly well suited to the determination of Γ_0/Γ. It would be much more satisfactory to obtain Γ_0/Γ from an independent measurement such as is available[32,33] for the 15.1-MeV level in C^{12}. Once the interpretation of inelastic electron scattering is established to be reliable, Γ_0/Γ may be inferred most conveniently by combining the value of Γ_0^2/Γ from elastic photon scattering with the value of Γ_0 inferred from inelastic electron scattering.

IV. DISCUSSION AND CONCLUSIONS

A. Comparison with Earlier Resonance Fluorescence Experiments

The results reported in this paper, obtained with better energy resolution than previously available, make it possible to reconcile the largest discrepancies in related, previously published results.[5–17] The data in Figs. 6–7 (together with unpublished data[34] showing a weaker level in Si somewhat below 11 MeV) make it clear that the previous resonant fluorescent experiments were mainly sensitive to the levels we report. The discrepancies between the energies we report for Mg and Si and those previously reported are not much outside of the experimental errors quoted by earlier investigators and might well be due to either the presence of several levels or reasonable calibration errors.

The discrepancies between the level parameters previously reported can also be understood to a large extent with the aid of the summary given in Table II. In the case of C^{12}, the discrepancies are relatively small. The measured integrated scattering cross sections are essentially within experimental error. (Note that we quote the value of 2.11 ± 0.31 MeV mb obtained from the scattering measurement in Ref. 6 rather than the value 2.33 ± 0.19 MeV mb, which includes the results of absorption measurements. Poor resolution absorption measurements seem to give too little absorption, as might be expected if there is some contribution from weaker, non-self-absorbing, levels; this smaller absorption, if interpreted in terms of a single level, implies a smaller value of Γ_0/Γ.) The main differences in the level parameters come from differences in the values inferred for Γ_0/Γ. However, the only way in which Γ_0/Γ can be measured precisely using only resonant absorption is with the aid of quite thick absorbers which accentuate any weaker levels that are present. With the absorber thickness we used, the inferred value of Γ_0/Γ was 1.0, but any value of Γ_0/Γ greater than 0.80 would have been consistent. To obtain level parameters, we used the value $\Gamma_0/\Gamma=0.96$ obtained from published experiments[32] which were sensitive to the 15.1- to 4.43-MeV cascade γ ray in C^{12}. This value of Γ_0/Γ assumes that the α-decay branch of the 15.1-MeV level is negligible; experiments sensitive to the α branch[33] indicate that it is less than 2% of the integrated scattering cross section. Our results are in good agreement with the more recent measurement made with $Li^7(p,\gamma)$ photons.[17]

The larger discrepancies between the reported level parameters for Mg and Si in Table II can also be understood to a large extent. First, it should be noted that there is not much disagreement between the measured values of the scattering cross section. (The discrepancies between these measurements might be due partly to the simultaneous sensitivity of the poor resolution experiments to several levels and partly to the lower priority previously given to the precise scattering measurement.) In addition, it should be noted that the extreme values of the level parameters given were caused more by different interpretation than by different measured values. In order to emphasize this, Table II presents the measured ratios of counts with and without different thicknesses of absorber. For comparison, the table also indicates the ratio expected on the basis of our level parameters, if only the strongest level were contributing. Table II illustrates clearly that the transmitted beam was always measured to be more intense than would be consistent with absorption by the single strong level; furthermore, the discrepancy is generally worse for a thicker absorber, as would be expected if scattering from weaker levels were playing a role. The main disagreement about level parameters was due to interpretation. In some cases[12,13] only one absorption measurement was made (i.e., no absolute scattering measurement was made), and the analysis assumed $\Gamma_0/\Gamma=1$. In these cases, the small values of Γ_0 listed in

[32] E. Almqvist, D. A. Bromley, A. J. Ferguson, H. E. Gove, and A. E. Litherland, Phys. Rev. 114, 1040 (1959); D. E. Alburger and R. E. Pixley, *ibid.* 119, 1970 (1960).

[33] Experiments using emulsions are quite sensitive to the three-α breakup of C^{12}, and a peaked contribution of 0.04 MeV mb would have been noticed. See, for example, M. E. Toms, Nucl. Phys. 50, 561 (1964). This implies that the alpha decay branch is less than 2%. A limit of 20% was set by G. L. Miller, R. E. Pixley, and R. E. Segel, Proc. Roy. Soc. (London) A259, 275 (1960).

[34] D. Drake, D. C. Sutton, and P. A. Tipler (private communication).

TABLE II. Comparison of resonance fluorescence results.

			C^{12}			
References	(a)	(b)	(c)	(d)	(e)	(f)
Γ_0 (eV)	37±5	54±9	59±10	54±6[g]	40±5	50±7[h]
Γ (eV)	39±5	79±16	64±10	60±8[g]	45±10	
$\int\sigma_S dE$ MeV mb	1.80±0.20	1.90±0.27	2.11±0.31	2.45±0.5[g]	1.82±0.12	

			Mg^{24}					
References	(a)	(i)	(d)				(j)	(k)
Γ_0 (eV)	17±4		137±40				4.8±1.6	3.8±1.2
Γ (eV)	21±4		980±280				l	l
$\int\sigma_S dE$ MeV mb	1.4±0.2	2.0±0.4	3.5±0.6				m	m
C_A/C_{NA}			0.83	0.71	0.54	0.48	0.77	0.71
C_A/C_{NA} predicted with our parameters			0.79	0.57	0.41	0.32	0.66	0.57

		Si^{28}				
References	(a)	(d)			(j)	(k)
Γ_0 (eV)	23±4	114±30			2.9±1.0	8.3±2.5
Γ (eV)	23±4	370±110			l	l
$\int\sigma_S dE$ MeV mb	2.0±0.3	6.2±1.0			m	m
C_A/C_{NA}		0.66	0.51	0.29	0.86	0.63
C_A/C_{NA} predicted with our parameters		0.55	0.38	0.23	0.60	0.53

[a] This experiment, assuming only strongest level contributes.
[b] Reference 5.
[c] Reference 6.
[d] Reference 9.
[e] Reference 17.
[f] Reference 16.
[g] Agreement with Refs. 5 and 6 was cited as a partial confirmation of calibration procedures.
[h] The quoted error assumes that four possible sources of 5% systematic errors would combine incoherently with the 5% statistical counting error. It is not clear that an error of 25% would contradict the reported results.
[i] Reference 8.
[j] Reference 12.
[k] Reference 13.
[l] $\Gamma_0=\Gamma$ was assumed.
[m] No measurement was made of absolute scattering.

Table II were inferred from the apparent small absorption. As Fig. 1 indicates, one would infer too large a value of Δ/Γ from too small an absorption (i.e., too small a slope in Fig. 1). On the other hand, Bussiere de Nercy[9] inferred particularly large level widths by combining measurements of angular distribution and scattered γ-ray line shape with absorption and absolute scattering measurements. In this case, the assumption that only a single level contributed led to unrealistically small values of Γ_0/Γ, which in turn would imply large values of both Γ_0 and Γ.

B. The Level Parameters and Their Implications

The 15.1-MeV Level in C^{12}

This well-studied level is the only one for which photon scattering measurements completely determine the parity as well as the spin; the angular distribution[35] of the scattered photons and the difference in azimuthal scattering caused by polarized photons[36] identify this magnetic dipole excitation. Our value of $\Gamma_0=37\pm5$ eV is in reasonable agreement with the values inferred from inelastic electron scattering: 41±7 eV,[19] 39±4 eV,[20] and 34.4±3.4 eV.[22] It also is quite close to the value of 32 eV predicted[37] by intermediate coupling fits to other data in the p shell.

The relatively large value of the magnetic dipole transition probability is interesting because it indicates that the 15.1-MeV level contains a large fraction of the strength of the "giant magnetic dipole resonance"[38] of C^{12}. If this strength is expressed in terms of the reduced transition probability $[b(M1)=(10\text{ MeV}/E)^3\ (\Gamma_0/11.6\text{ eV}]$, $b(M1)=0.928$ for $\Gamma_0=37$ eV [see Eq. (19) below]. It should be emphasized that so large a value of b implies the cooperative behavior of several nucleons.[38] In this case, the usual "single-particle unit" $b_u(M1)=1.79$ might be misleading because it overestimates the transition probability associated with most single particle orbits.

The value of Γ_0 for this level is especially important because it plays a role in the test of the conserved vector current theory of β decay[39] which involves the shape-dependent factors in the β spectra of B^{12} and N^{12}. The value of $A+\delta A=(1.10\pm0.17)\%$ per MeV used to compare the experiment was based[40] on $\Gamma_0=50$ eV; if Γ_0 is taken as 37 eV, $A+\delta A$ becomes $(0.91\pm0.17)\%$ per MeV while the experimental values are (1.30

[35] J. E. Leiss and J. M. Wyckoff, Bull. Am. Phys. Soc. **1**, 21 (1956).
[36] D. Jamnik and P. Axel, Phys. Rev. **117**, 194 (1960).
[37] S. Cohen and D. Kurath, Nucl. Phys. **73**, 1 (1965).
[38] D. Kurath, Phys. Rev. **130**, 1525 (1963).
[39] M. Gell-Mann, Phys. Rev. **111**, 362 (1958).
[40] T. Mayer-Kuckuk and F. C. Michel, Phys. Rev. **127**, 545 (1962).

± 0.31),[40] (1.62 ± 0.28),[41] and (1.19 ± 0.24),[42] later revised to (1.07 ± 0.24).[43]

The 9.92 and 10.66 MeV Levels in Mg^{24}

The dipole character of the photon transition of the stronger 10.66-MeV level follows from the angular distribution[9] while its assignment as magnetic dipole depends on electron scattering.[21,23] The magnetic dipole character of the 9.92-MeV level can be based on either the high-resolution electron scattering[23] or on analog-state systematics as will be discussed below. The width of 17 eV quoted in Table I should have an error of about ± 2.5 eV assigned to it if $\Gamma_0/\Gamma=0.8$; the good-resolution electron-scattering result[23] is $\Gamma_0=22.2\pm 2.4$ eV. (The earlier poorer-resolution result was 21 eV,[21] but was recalculated to be 34 eV using a different transition radius.[23]) The results almost overlap, and they would agree completely if Γ_0/Γ were as low as 0.61. For the 9.92-MeV level, our value of $\Gamma_0=5.6$ eV would have about a 1-eV error if Γ_0/Γ were 0.54. If Γ_0/Γ were taken as 0.38, which is within the limit of our error, our value of Γ_0 would become 7.9 eV compared with the value of 7.95 ± 1.2 eV assigned to an unresolved doublet at 9.85 and 9.97 MeV from electron scattering.[23] Our values for the 9.92- and 10.66-MeV levels correspond to $b(M1)$ values of 0.49 and 1.21, respectively.

There are other nuclear reactions which probably give information about the 10.66- and 9.92-MeV levels we observe. Levels in Mg^{24} have been reported[44] at 10.66 ± 0.02 MeV and 9.960 ± 0.015 MeV on the basis of the $Na^{23}(He^3,d)$ reaction. As will be discussed below, the levels we see are probably intimately related to low lying levels in Na^{24} which are well represented by Na^{23} plus one nucleon, and hence should be strongly excited in an $Na^{23}(He^3,d)$ reaction. What appears to be these same levels have been fit into decay schemes[45,46] derived from the γ-ray cascade following proton capture by Na^{23}. (These decay schemes show an inconsistently small γ-ray branch from the 10.66 level to the ground state, but it is possible that γ rays from stronger branches of the cascade obscured the 10.66-MeV γ rays which dominate the decay of the level we observed.)

The 10.07-MeV Level in Mg^{26}

Our original assignment of the 10.07-MeV level to Mg^{26} was based on the occurrence of a 10.08-MeV γ ray, assigned[47] to Mg^{26}, in the capture of neutrons by Mg. A level at 10.09 MeV (as well as at 10.03 and 10.12 MeV) was also reported in the $Al^{27}(t,\alpha)$ reaction.[48] The same level has been seen and identified as $M1$ in inelastic electron scattering from isotopically enriched Mg^{26}; the reported energies are about 10.2 MeV [23] and 10.1 MeV.[24] From our value of $\Gamma_0^2/\Gamma=4.2$ eV, the $b(M1)$ value must be 0.36 if $\Gamma_0/\Gamma=1$, and greater otherwise.

The 11.42-MeV Level in Si^{28}

The dipole character of the transition to this energy level can be based on the observed distribution of scattered γ rays.[9] The assignment as magnetic dipole was based on the inelastic-electron-scattering results.[19,20] The width we determined was 23 eV with an error of about 3.5 eV if $\Gamma_0/\Gamma=1$. The poor-resolution electron-scattering experiments gave 47 eV with a 30% error[19] and 33 eV with a 40% error.[20] The level was also seen in good resolution by the Darmstadt group,[49] but they have not yet published detailed parameters. Our value of 23 eV corresponds to a $b(M1)$ of 1.33.

An 11.40-MeV level had been reported[45] in a γ-ray cascade following the capture of 1.117-MeV protons by Al. An 11.40-MeV level was also invoked[50] to explain a weak branch in the γ cascade following the capture of a 2.522-MeV proton. Very strong 11.4-MeV γ rays were also seen[50] in the cascades following the capture of 1.669- and 1.680-MeV protons, but these were interpreted as decays from the capturing state to the first $2+$ state in Si^{28}.

C. Identification of Analog States and the Giant Magnetic Dipole Resonance

The identification of the transitions as magnetic dipole and the large transition strength associated with the levels at 9.92 and 10.66 MeV in Mg^{24} and at 11.42 MeV in Si^{28} indicates that these levels are dominantly $T=1$, in accordance with the rule first discussed by Morpurgo.[51] If only the integrated strength associated with each level had been measured, the possibility would remain that what appeared as a single strong level with our 100-keV resolution was actually a group of weaker levels. (This type of fragmentation of an analog state has been demonstrated in the high-resolution examination[52] of analog states near 10 MeV in K^{41}.) However, our resonant absorption results make it clear that the strength associated with each of the

[41] N. W. Glass and R. W. Peterson, Phys. Rev. **130**, 299 (1963).
[42] Y. K. Lee, L. W. Mo, and C. S. Wu, Phys. Rev. Letters **10**, 253 (1963).
[43] C. S. Wu, Rev. Mod. Phys. **36**, 618 (1964).
[44] S. Hinds and R. Middleton, Proc. Phys. Soc. (London) **76**, 553 (1960).
[45] P. M. Endt and C. Van der Leun, Nucl. Phys. **34**, 1 (1962).
[46] P. W. M. Glaudemans and P. M. Endt, Nucl. Phys. **42**, 367 (1963).
[47] P. J. Campion and G. A. Bartholomew, Can. J. Phys. **35**, 1361 (1957).
[48] S. Hinds, H. Marchant, and R. Middleton, Proc. Phys. Soc. (London) **78**, 473 (1961).
[49] P. Brix, H. G. Clerc, R. Engfer, G. Fricke, F. Gudden, H. Liesem, and E. Spamer, in *Comptes Rendus du Congres International de Physique Nucleaire, Paris, 1964* (Editions du Centre National de la Recherche Scientifique, Paris, 1965), Vol. II, p. 372.
[50] Y. P. Antoufiev, D. A. E. Darwish, O. E. Badawy, L. M. El-Nadi, and P. V. Sorokin, Nucl. Phys. **56**, 401 (1964).
[51] G. Morpurgo, Phys. Rev. **110**, 721 (1958).
[52] G. A. Keyworth, G. C. Kyker, Jr., E. G. Bilpuch, and H. W. Newson, Nucl. Phys. **89**, 590 (1960); Phys. Letters **20**, 281 (1966).

three strong levels is not significantly fragmented. Thus, there is no evidence for significant mixing between $T=1$ 1+ states and any $T=0$ 1+ states that might exist at excitations of about 10 MeV in Mg^{24} and Si^{28}. The lack of mixing between $T=1$ and $T=0$ 1+ levels requires that the $T=0$ 1+ levels be well separated. This is consistent with the apparent isolated levels observed[45] in a wide variety of experiments in Mg and Si near 11 MeV. On the other hand, the widely spaced levels are quite inconsistent with the strong absorption of bremsstrahlung γ rays reported[53] near 11 MeV in Mg, but consistent with the negligible absorption reported[54] for both Mg and Si in a similar experiment.

The identification of strong $T=1$ 1+ states in Mg^{24} and Si^{28} can be used together with known Coulomb energies to predict the presence of low-lying 1+ states in Na^{24} and Al^{28}, respectively. This relation between the low 1+ states (in Na^{24} and Al^{28}) and the strong scattering levels (in Mg^{24} and Si^{28}) was recognized by Sugawara,[13] but he did not have sufficiently precise information to make exact identifications.

The nuclear-structure implications of the observed magnetic dipole transition strengths can be understood more readily if one uses the approximate (but probably rather accurate) sum rule for $A=4N$ nuclei given by Kurath[38]:

$$\sum_j \left[\frac{\Gamma_{0j}(M1)}{3.395\text{ eV}}\right]\left(\frac{10\text{ MeV}}{E_j}\right)^2=\left(\frac{-a}{2\text{ MeV}}\right)\times\langle g|\sum_i \mathbf{l}_i\cdot\mathbf{s}_i|g\rangle. \quad (17)$$

$\Gamma_{0j}(M1)$ is the magnetic dipole transition width from the excited state j to the ground state g. E_j is the excitation energy of the jth state. The quantity a is the coefficient of the $\mathbf{l}_i\cdot\mathbf{s}_i$ term in the potential of the ith nucleon; for the d shell, $a\simeq-2$ MeV. Equation (17) is obtained directly from Eq. (8) of Ref. 38 by substituting the experimental values of μ_N and μ_P. Equation (17) has the advantage of being expressed in terms of the width rather than the reduced width $B(M1)$ which is sometimes defined somewhat differently by different authors.

The Weisskopf unit for $\Gamma_0(M1)$ is $\Gamma_{0\text{W.u.}}(M1)=20.7$ eV $(E/10\text{ MeV})^3$ while the Moszkowski unit is $\Gamma_{0\text{M.u.}}(M1)=19.3\ (E/10\text{ MeV})^3$. Inasmuch as $\langle\mathbf{l}\cdot\mathbf{s}\rangle=\frac{1}{2}l$ for a particle in the $j=l+\frac{1}{2}$ state, Eq. (17) clearly indicates that the Weisskopf or Moszkowski unit is about a factor of 6 larger than would be expected for a pure single-particle transition. $B(M1)$ is often used in place of Γ_0. We use the conventional definition[55] of $B(M1)$:

$$\Gamma(M1)=(16\pi/9)(E/\hbar c)^3B(M1). \quad (18)$$

It is convenient to define a dimensionless quantity $b(M1)$ by the relation

$$B(M1)=b(M1)(e\hbar/2M_pc)^2, \quad (19)$$

where M_p is the proton mass. Substituting Eq. (19) in Eq. (18) gives

$$\Gamma(M1)=11.58\text{ eV}(E/10\text{ MeV})^3b(M1). \quad (20)$$

[The factor called $B(M1)$ in Ref. 38 is the same as the factor called $\Lambda(M1)$ in Ref. 37, and is $\frac{4}{3}\pi b(M1)$.] The conventional Weisskopf and Moszkowski units correspond to $b_{\text{W.u.}}(M1)=1.79$, $\Lambda_{\text{W.u.}}(M1)=7.50$, $b_{\text{M.u.}}=1.67$, and $\Lambda_{\text{M.u.}}(M1)=6.99$.

In order to apply Eq. (17) to C^{12}, one should note that the observed spin-orbit splitting for the p shell corresponds to $a\simeq-4.2$ MeV. Thus, from Eq. (17), the measured value of $\Gamma=37$ eV implies $\langle\sum_i \mathbf{l}_i\cdot\mathbf{s}_i\rangle=2.29$, whereas if there were 8 $p_{3/2}$ nucleons, one would expect $\langle\sum_i \mathbf{l}_i\cdot\mathbf{s}_i\rangle=4.0$. If C^{12} were believed to be a pure j-j coupled nucleus with a filled $p_{3/2}$ shell, Eq. (17) would imply that there was substantial additional magnetic dipole transition strength. However, the systematic behavior of the intermediate coupling parameter in the p shell[37] implies that the 15.1-MeV level in C^{12}, with a predicted width of 32 eV, is essentially the entire giant magnetic resonance.[38]

In the case of Mg^{24} our values inserted into Eq. (17) imply $\langle\sum_i \mathbf{l}_i\cdot\mathbf{s}_i\rangle=6.08$. In the spherical j-j coupled shell model, this value could be understood if six of the eight nucleons beyond the O^{16} core were in the $d_{5/2}$ state, while the other two were in the $s_{1/2}$ orbit. Even if there were eight $d_{5/2}$ nucleons in Mg^{24}, the levels we see form a substantial part of the giant dipole. However, this interpretation implies that the excited 1+ state is dominantly $(d_{5/2})^{-1}d_{3/2}$, which would be unexpected as a low-lying configuration in Na^{24} because the $s_{1/2}$ and $d_{5/2}$ subshells are not filled. Assuming that the 9.51-MeV level in Mg^{24} is properly identified[56] as the lowest $T=1$ state, our data imply 1+ states in Na^{24} at about 0.41 MeV and 1.15 MeV, compared with the known states at 0.47 MeV and 1.35 MeV.

A more consistent interpretation of the 1+ levels can be obtained by using the Nilsson[57] model orbitals as was done in some detail by Daum.[58] This model implies that the $220+[Nn_z\Lambda\Sigma]$ state (Nilsson orbit 6) and the 211+ state (Nilsson orbit 7) are filled in the ground state of Mg^{24}, while the 202+ state (orbit 5) and the 211− state (orbit 9) are the next available vacant states. It is very attractive to associate the ground state (4+) and first excited state (1+) of Na^{24} with the

[53] B. S. Dolbilkin, V. I. Korin, L. E. Lazareva, F. A. Kikolaev, and V. A. Zapevalov, Nucl. Phys. **72**, 137 (1965).
[54] J. M. Wyckoff, B. Ziegler, H. W. Koch, and R. Uhlig, Phys. Rev. **137**, B576 (1965).
[55] K. Alder, A. Bohr, T. Huus, B. Mottelson, and A. Winther, Rev. Mod. Phys. **28**, 432 (1956).
[56] M. Rickey, E. Kashy, and D. Knudsen, Bull. Am. Phys. Soc. **10**, 550 (1965).
[57] S. G. Nilsson, Kgl. Danske Videnskab. Mat. Fys. Medd. **29**, No. 16 (1955).
[58] C. Daum, Nucl. Phys. **51**, 44 (1964).

spin-parallel and spin-antiparallel coupling of a 211+ proton with a 202+ neutron. The assignment of the same configuration to these two levels is consistent with the fact that their relative spacing changes relatively little when the neutron is changed into a proton in going from Na^{24} to Mg^{24}. (The 0.47-MeV spacing in the Na^{24} is to be compared to the 0.41- or 0.45-MeV spacing in Mg^{24} depending on whether the level is at 9.92 or 9.96 MeV.) The second 1+ state in Na^{24}, seems to be consistent with a dominant configuration of a 211+ proton coupled to a 211− neutron.[58] This is consistent with the fact that the 211− assignment seems appropriate for the first excited state of both Mg^{25} and Al^{25} which have a ground state consistent with 202+. In going from Mg^{25} to Al^{25} the 202+ state moves up relative to the 211− state by 120 keV; according to the assignments proposed above for Na^{24} and Mg^{24}, the state involving the 202+ orbit moves up relative to the one with the 211− orbit by 200 keV. Although the understanding of the energy shift requires detailed calculations, it seems reasonable to find the shift in the same direction in the $A=24$ and $A=25$ systems.

The assignments of the dominant configurations of the two 1+ states in Mg^{24} are also supported by the relative size of the magnetic dipole transition moments. The first 1+ state, which has the dominant configuration $(211+)^{-1}$ 202+, can be reached by a magnetic dipole transition only by the orbital angular-momentum operator of the proton, whereas the $(211+)^{-1}$ (211−) state can be reached by the spin-flip operator acting on both neutrons and protons. The value of $\langle\sum_i \mathbf{l}_i\cdot\mathbf{s}_i\rangle$ is, according to the Nilsson model (with a prolate deformation $\eta=4$), 6.04 which is very close to the experimental value of 6.08 (if $a=-2$ MeV).

Theoretical calculations have shown that the Mg^{24} nucleus may be axially asymmetric as well as deformed.[59] The wave functions given by these calculations indicate that Mg^{24} deviates from a prolate shape somewhat, and corresponds to a $\langle\sum_i \mathbf{l}_i\cdot\mathbf{s}_i\rangle$ of only 3.33, in contrast with the observed, higher, result. It is not clear to what extent more detailed calculations, including both pairing and configuration mixing, might change these predictions; but until such refinements change the predictions (as is likely), the experimental data reported in this paper are more consistent with the simpler axially symmetric deformed nuclear model.

Although there are less data available on the Al^{28}-Si^{28} nuclei, some comparisons can be made. The single level at 11.42 MeV inserted in Eq. (17) implies a value of $\langle\sum_i \mathbf{l}_i\cdot\mathbf{s}_i\rangle$ of about 5.2. (The weaker level observed near 10.9 MeV [34] will increase this value somewhat.) Inasmuch as Si^{28} has 12 particles beyond the O^{16} core, the spherical j-j coupled model could explain a value between 8 and 12, depending on the extent to which the $d_{5/2}$ and $s_{1/2}$ orbits are filled. However, once again, the low excitation energy of the corresponding 1+ states in Al^{28} argues against an assignment of $(d_{5/2})^{-1}d_{3/2}$ even though this assignment is required for a strong magnetic dipole transition.

The level at 11.42 MeV in Si^{28} implies a 1+ excited state in Al^{28} near 2.11 MeV, assuming that the analog of the Al^{28} ground-state doublet is[45,56,60] at 9.31 and 9.38 MeV in Si^{28}. It seems reasonable that the 2.147-MeV level in Al^{28} is the 1+ level, particularly because it participates[45] in the neutron capture γ-ray cascade as does the identified 1+ state at 1.37 MeV. (The 2.209-MeV level in Al^{28} does not seem to participate in the γ-ray cascade, while the evidence about the 2.281-MeV level is ambiguous. If the 2.281-MeV level were the implied 1+ state, its position above the ground state of Al^{28} would be about 170 keV higher than the corresponding level in Si^{28}. This shift seems large relative to the position of the first 1+ level in Al^{28}, which at 1.37 MeV is itself about 220 keV below the energy implied by the 10.9-MeV level[34] in Si^{28}, if it is a magnetic dipole transition. The weakness of any magnetic dipole strength at 10.7 MeV and the strength of the transition to the 10.9-MeV region casts doubt on the $T=1$ assignment tentatively suggested[45,60] for the 10.7-MeV level in Si^{28}.)

As Kurath originally pointed out, a study of the main magnetic dipole transition strengths in Si^{28} might help decide about whether the oblate or prolate shape was more consistent with a deformed axially symmetric model. Unfortunately, the oblate prediction[57] of $\langle\sum_i \mathbf{l}_i\cdot\mathbf{s}_i\rangle=7.6$ and the prolate prediction of 4.3 (for $\eta=-4$) bracket the experimental sum which will be somewhat greater than 5.2. Furthermore, another axially symmetric oblate solution,[59] gives a value of only 4.3 instead of 7.6, indicating an embarrassing sensitivity of the $\langle\sum_i \mathbf{l}_i\cdot\mathbf{s}_i\rangle$ to calculational details. For completeness, it might be indicated that the suggested non-axially-symmetric deformed solution[59] for Si^{28} gives $\langle\sum_i \mathbf{l}_i\cdot\mathbf{s}_i\rangle=6.2$.

In addition to being helpful in assigning the spin of one of the Al^{28} levels, the strong magnetic dipole transition will provide information about the configuration. For example, if the Si^{28} ground state has the 202 $\frac{5}{2}$ orbit filled, the 11.42-MeV level must have an important component which can be reached by a spin flip such as $(202+)^{-1}$ (202−). There is also the possibility that the 11.42 level is a coherent mixture of $(202+)^{-1}$ (202−) and $(211+)^{-1}$ (211−).

Although the magnetic transition strengths we found in Mg^{24} and Si^{28} do not exhaust the entire sum rule of Eq. (17) in the spherical strong j-j coupled shell model, at a very minimum they include a substantial fraction of the entire sum. More probably, the transitions we observe come close to accounting for the entire sum predicted by better nuclear models for the ground state

[59] J. Bar-Touv and I. Kelson, Phys. Rev. 138, B1035 (1965).

[60] P. M. Endt and A. Heylingers, Physica 26, 230 (1960).

of these nuclei. (The absence of additional strong magnetic dipole transitions in inelastic electron scattering tends to reinforce this conclusion.) While the qualitative size of the magnetic transition probability and the division of strength between two levels in Mg^{24} can be understood in terms of the asymptotic quantum numbers of an axially symmetric deformed nuclear model, a more quantative interpretation will require calculations of the effects of pairing on the ground states of Mg^{24} and Si^{28} and the effects of configuration mixing on the excited 1+ states.

Note added in proof: The giant magnetic dipole resonance in the (*s*,*d*) shell, and its influence on the inelastic scattering of high energy protons, were treated by Kawai *et al.*[61]

The two γ rays of Mg^{24} were recently seen by Riess *et al.*,[62] who report energies of 10.03±0.06 and 10.80±0.10 MeV.

ACKNOWLEDGMENTS

The authors are indebted to Dr. Dieter Kurath and Dr. B. R. Mottelson for stimulating, informative discussions.

[61] M. Kawai, T. Terasawa, and K. Izumo, Nucl. Phys. **59**, 289 (1964).

[62] F. Riess, W. J. O'Connell, D. W. Heikkinen, H. M. Kuan, and S. S. Hanna, Phys. Rev. Letters **19**, 367 (1967).

PHYSICAL REVIEW VOLUME 163, NUMBER 4 20 NOVEMBER 1967

Alpha Decay of Holmium Nuclei; New Isotope, ^{154}Ho†

R. L. Hahn, K. S. Toth, and T. H. Handley
Oak Ridge National Laboratory, Oak Ridge, Tennessee

(Received 12 June 1967)

Neutron-deficient holmium isotopes were produced by $^{156}Dy(p,xn)$ reactions. Chemical separations verified that the products were holmium nuclei; excitation-function determinations served to assign mass numbers to them. A new isotope, ^{154}Ho, was found to emit α particles of 3.91±0.02 MeV with a half-life of 11.8±1.0 min. A search was made for an α-decay transition from ^{155}Ho, but none was observed. The radionuclides ^{153}Ho and ^{152}Ho, already known to exist, were found to have respective α energies and half-lives that were 3.97±0.02 MeV and 9.3±0.5 min, and 4.37±0.02 MeV and 2.7±0.2 min. For ^{153}Ho, the α-decay-to-electron-capture ratio was measured to be $(1.2\pm0.7)\times10^{-3}$. From a comparison with semiempirical estimates of α-decay rates, it was concluded that the α transition of ^{153}Ho is not hindered.

I. INTRODUCTION

THE study of the α decay of neutron-deficient isotopes with neutron numbers between 84 and 88 is of interest because of its pertinence to the systematics of α decay. Because of the stable closed-shell configuration for 82 neutrons, the α-decay energies of these nuclei are enhanced and, moreover, decrease rapidly with increasing neutron number (above 84).[1]

Several α-emitting holmium nuclides in this neutron range are known. Unfortunately, there are conflicting reports in the literature about the characteristics of their decay modes. Macfarlane and Griffioen,[2] in an extensive study of the $^{141}Pr(^{16}O,xn)$ reactions leading to various holmium radionuclides, reported on the decay properties of the mass 151, 152, and 153 isotopes; in particular, 9±2 min ^{153}Ho was found to emit an α particle of 3.92 MeV. In this same work, they stated that they were not able to corroborate the preliminary results[3] they had earlier reported for ^{154}Ho and ^{155}Ho; no α activities for masses greater than 153 could be found. Nevertheless, compilations of nuclear data[4,5] still contain some of the early results later retracted by Macfarlane and Griffioen.

In addition, May and Yaffe,[6] in a radiochemical investigation of the reactions of dysprosium with protons, concluded that the 27-min component that they observed was possibly ^{153}Ho. And, recently Lagarde *et al.*[7] assigned a half-life of 7±1 min to ^{154}Ho.

In an attempt to resolve some of the reported discrepancies, we have investigated the α-particle spectra from the products of the $^{156}Dy(p,xn)^{(157-xn)}Ho$ reactions. We shall herein report on the α-particle energies and half-lives that were determined, and on the excitation-function measurements so necessary for unequivocal mass assignments of the observed radionuclides.

† Research sponsored by the U. S. Atomic Energy Commission under contract with the Union Carbide Corporation.

[1] V. E. Viola, Jr., and G. T. Seaborg, J. Inorg. Nucl. Chem. **28**, 697 (1966).

[2] R. D. Macfarlane and R. D. Griffioen, Phys. Rev. **130**, 1491 (1963).

[3] R. D. Macfarlane and R. D. Griffioen, Bull. Am. Phys. Soc. **6**, 287 (1961).

[4] *Nuclear Data Sheets*, compiled by K. Way *et al.* (Printing and Publishing Office, National Academy of Sciences–National Research Council, Washington, D. C., 1965), NRC 5-5-26, 5-6-59, 5-5-51.

[5] *Chart of the Nuclides*, compiled by D. T. Goldman and J. R. Roesser (Knolls Atomic Power Laboratory, 1966).

[6] M. May and L. Yaffe, J. Inorg. Nucl. Chem. **26**, 479 (1964).

[7] P. Lagarde, J. Tréherne, A. Gizon, and J. Valentin, J. Phys. (Paris) **27**, 116 (1966).